Jurnal Kejuruteraan 38(2) 2026: 649-662
https://doi.org/10.17576/jkukm-2026-38(2)-15

Modelling and Verification of Tractor–Semitrailer Hitch Joint via Kinetic Equations of Motion Based on the Virtual Dugoff Tire Model Approach

Amrina Rasyada Zubir[a], Mohamad Hafiz Harun[a*], Fauzi Ahmad[a] & Ubaidillah Sabino[b]

[a]*Faculty of Mechanical Technology and Engineering, Universiti Teknikal Malaysia Melaka, Hang Tuah Jaya, 76100 Durian Tunggal, Melaka, Malaysia.*

[b]*Faculty of Engineering, Universitas Sebelas Maret, Kota Surakarta, 57126 Jawa Tengah, Indonesia.*

[*]*Corresponding author: mohamadhafiz@utem.edu.my*

Received 20 July 2025, Received in revised form 3 December 2025
Accepted 3 January 2026, Available online 30 March 2026

ABSTRACT

The hitch joint plays a critical role in heavy vehicles, serving as the primary linkage between the tractor and the semitrailer. To replicate accurately the behavior of an actual tractor–semitrailer system, it is necessary to consider the full range of kinematic and dynamic interactions acting on this joint. Previous hitch joint modeling approaches often relied on the Pacejka Magic Formula, which, although accurate, requires extensive parameter tuning and imposes high computational demand, making it inconvenient for real-time applications. This research addresses the limitation by developing a novel hitch joint model based on the Dugoff tire formulation, a well-established technique in vehicle dynamics for simulating nonlinear tire behavior. Compared to the widely used Pacejka Magic Formula, the Dugoff model offers simpler implementation while maintaining competitive accuracy. The proposed hitch joint model was combined with a 12-degree-of-freedom (DOF) tractor-semitrailer handling model, where maneuverability predictions were evaluated using Double Lane Change (DLC) and Step Steer Cornering (SSC) tests, and verified using the validated simulation software, TruckSim. Simulation results demonstrated strong agreement between the proposed model and the validated TruckSim model, with average percentage differences in root mean square (RMS) values of 3.141% and 1.830% for the DLC and SSC tests, respectively. These findings confirm that the proposed hitch joint model can serve as a reliable dynamic representation for future applications in heavy-vehicle design optimization, handling control development, and rollover stability evaluation.

Keywords: Tractor-semitrailer; Hitch joint model; double lane change; step steer cornering; Dugoff tire model

INTRODUCTION

Commercial vehicle accidents have become a prominent topic in the media due to the significant impacts often witnessed in these incidents, particularly involving tractor-semitrailer drivers who transport heavy loads using articulated vehicles. These vehicles are at a high risk of experiencing rollover incidents due to various factors, such as braking, cornering, and loading distribution (Ikhsan et al. 2021; Zainuddin et al. 2023). To address these issues, a rollover warning system has been introduced, using a similar approach to the advanced driver-assistance systems (ADAS) found in standard vehicles. This system is grounded in dynamic modeling of the tractor semi-trailer, considering the forces, as well as the kinetic and potential energies, affecting the vehicle body (Harun et al. 2021). There are three common methods for multibody modeling of a tractor-semitrailer: the first is a simpler approach using MATLAB/Simulink; the second is a more advanced technique employing MSC. ADAMS by McNeil Schindler Corp (MSC) in 2002; and the third involves co-simulation using several configurations, such as ADAMS and MATLAB/Simulink, or MATLAB/Simulink in combination with TruckSim, to assess the performance of heavy vehicle handling control systems. These hybrid models have been shown to significantly reduce the tendency for rollover (Hafez 2021; Assadi et al. 2024).

MATLAB/Simulink provides an accurate yet simplified modeling environment that enables rapid processing and fast system response by deriving equations of motion using Newton's second law or Lagrange's equations (Blight et al. 2021). The truck's dynamics can be represented in quarter, half, or full configurations, allowing flexibility in ride and handling analysis (Hamza et al. 2024). According to Hwang et al. (2020), these configurations take inputs such as acceleration, velocity, and displacement to improve the model's accuracy in predicting the truck's behavior. On the other hand, deriving complex equations and matrix-based solutions for higher-fidelity models requires significantly greater computational power and time (Lu et al. 2022). Therefore, such detailed derivations are better suited for applications requiring high precision, where accurate parameter prediction is essential. Consequently, this rationale supports the choice of the latter option.

Automated dynamic analysis of mechanical systems (ADAMS) offers a 3D graphical representation of multibody dynamics (MBD), which can significantly reduce model complexity by parameterizing elements such as masses, stiffnesses, and damping coefficients, connected via linkages and contacts, making it especially useful for kinematic analysis and dynamic studies (Linden, 2020). For instance, Henrique et al. (2023) examined the effectiveness of multibody modeling in estimating lateral load transfer ratios, concluding that full-vehicle simulations in ADAMS provided more reliable stability assessments than lumped-mass models alone. This approach avoids the computational expense of a full finite element analysis (FEA). However, in cases where the fatigue or dynamics of flexible components are critical, integrating FEA within the MBD framework enhances accuracy, as it allows for a comprehensive assessment across a full range of motion and varying operating environments, thereby improving the reliability of FEA results (Hexagon AB, 2024).

In this study, a comprehensive truck model was developed by integrating a 12-degree-of-freedom (DOF) tractor handling model with a hitch joint model, representing the connection to the trailer component. The equations of motion for the tractor body kinematics were derived, and handling tests were simulated using MATLAB/Simulink. To assess the model's accuracy, the results were compared with those from the validated TruckSim model by performing two specific tests: the double lane change (DLC) and steep steer cornering (SSC) tests. Accurate characterization of these dynamic interactions formed the analytical foundation for rollover warning systems, where lateral acceleration, yaw rate, and hitch load responses served as the main indicators of rollover risk. Hence, this model supports the development of predictive rollover indices and stability-control algorithms for articulated vehicles. This refined modeling approach aimed to provide a more accurate representation of tractor–semitrailer dynamics compared to existing hitch joint models, which often neglect the nonlinear tire–road interactions that significantly influence the behavior of articulated vehicles.

The Dugoff tire model, adopted in this study, effectively captured variations in tire stiffness and rolling radius during critical events such as tire blowouts or sudden steering maneuvers. Compared to more complex formulations, such as the Pacejka Magic Formula, which require extensive parameterization and impose higher computational costs, the Dugoff model offers comparable dynamic accuracy while providing enhanced real-time responsiveness and reduced implementation complexity. This manuscript is organized as follows: Section 1 introduces the main components of the rollover warning system, emphasizing the modeling process and presenting a recent review of related work in this field; Section 2 details the derivation of the equations of motion for both the tractor-semitrailer and hitch joint models, including the fifth-wheel coupling; Section 3 presents model verification results obtained from TruckSim simulations; and Section 4 concludes with a discussion of the key findings and their implications.

METHODOLOGY

MATHEMATICAL MODELLING OF TRACTOR-SEMITRAILER WITH HITCH JOINT

This study aimed to develop a comprehensive modeling of a 12-DOF full truck model, focusing on a critical configuration of a tractor-semitrailer system. The configuration consisted of a two-axle tractor, a hitch, and a single-axle semitrailer, as illustrated in Figure 1. Both the tractor and semitrailer underwent dynamic modelling, incorporating internal forces and momentum to accurately capture the vehicle's response, including lateral, longitudinal, and yaw motions (Kabbani et al. 2023). The model also accounted for the nonlinear tire forces generated through the rotational motion of each wheel, which was treated as an additional single rotational degree of freedom (1-DOF) per tire in the tire-force submodel. However, these wheel rotations were embedded within the tire dynamics and did not increase the overall system's 12-DOF formulation. For the hitch joint, a kinematic approach was used to describe the vehicle's lateral velocity, acceleration, and yaw relative to the vehicle's local coordinate system.

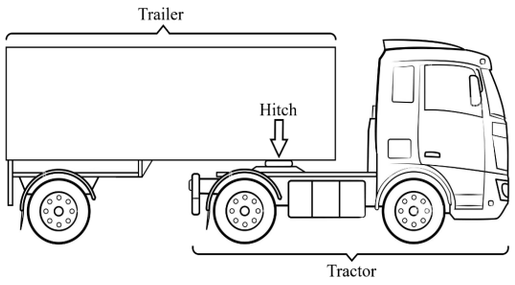

FIGURE 1. Configuration of a 3-axle tractor-semitrailer

DERIVATION OF 7-DOF TRACTOR MODEL

In this study, the equations of motion for a two-axle tractor model were developed by accounting for the vertical forces acting on the tires and the hitch, derived with respect to the tractor's center of gravity, as shown in Figure 2. Additionally, the rotational motions of the tractor body and wheels were formulated using a tractor handling model, integrating both local and global positioning systems. This model allows the tractor to move freely in the lateral and longitudinal directions and to rotate about the vertical axis, while road surface friction is neglected (Adnan et al. 2023).

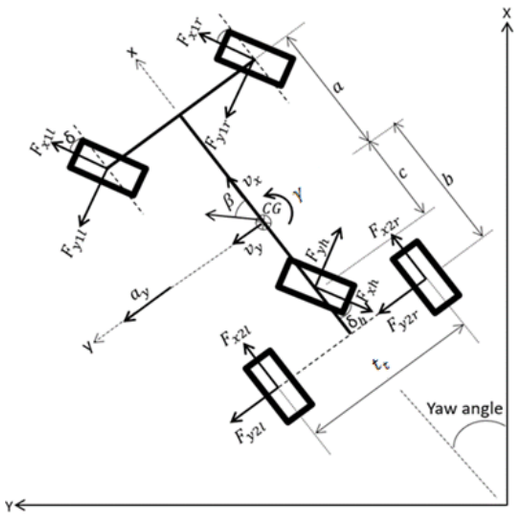

FIGURE 2. Two-axle tractor handling model

To determine the vertical tire-load distribution on the tractor, the vehicle was analyzed while moving on an inclined plane. This simplified condition allows all vertical, longitudinal, and hitch-induced forces to be projected with respect to the slope angle, which is essential for deriving the static and dynamic equilibrium equations. Accordingly, Figure 3 illustrates the free-body diagram of the tractor on an inclined ramp, from which the balance of weight, inertia-induced moments, and hitch reactions is established to derive Equations (1)–(4).

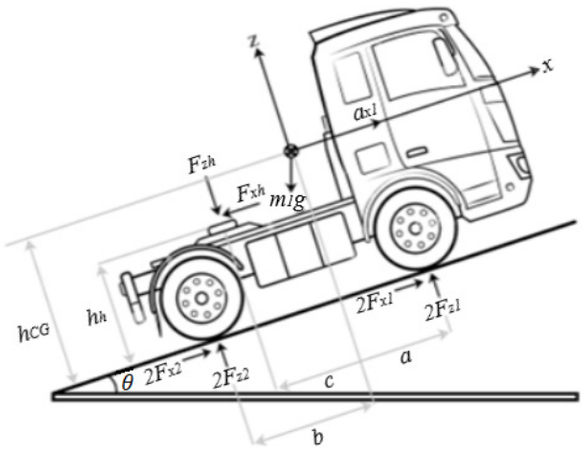

FIGURE 3. Free-body diagram of a tractor on an inclined ramp

$$+\circlearrowleft M = F.d, \sum M_{axle,tractor} = 0$$

$$F_{z1,r} = \frac{1}{a+b}\begin{pmatrix} m_1 g cos\theta . b - m_1 g sin\theta . h_{CG} \\ +m_1 a_{x1} . h_{CG} + F_{zh}(b-c) \\ -F_{xh} . h_h + m_1 a_y . h_{CG} \end{pmatrix} \quad (1)$$

$$F_{z1,l} = \frac{1}{a+b}\begin{pmatrix} m_1 g cos\theta . b - m_1 g sin\theta . h_{CG} \\ +m_1 a_{x1} . h_{CG} + F_{zh}(b-c) \\ -F_{xh} . h_h - m_1 a_y . h_{CG} \end{pmatrix} \quad (2)$$

$$F_{z2,r} = \frac{1}{a+b}\begin{pmatrix} m_1 g cos\theta . a + m_1 g sin\theta . h_{CG} \\ -m_1 a_{x1} . h_{CG} + F_{zh}(a+c) \\ +F_{xh} . h_h + m_1 a_y . h_{CG} \end{pmatrix} \quad (3)$$

$$F_{z2,l} = \frac{1}{a+b}\begin{pmatrix} m_1 g cos\theta . a + m_1 g sin\theta . h_{CG} \\ -m_1 a_{x1} . h_{CG} + F_{zh}(a+c) \\ +F_{xh} . h_h - m_1 a_y . h_{CG} \end{pmatrix} \quad (4)$$

Based on these equations, $F_{z1,r}$ and $F_{z1,l}$ represent the vertical tire forces at the front axle on the right and left sides, respectively, while $F_{z2,r}$ and $F_{z2,l}$ represent the vertical tire forces at the rear axle on the right and left sides, respectively. F_{zh} is the vertical force, and F_{xh} is the longitudinal force at the hitch. m_1 is the mass of the tractor, g is the gravitational acceleration, θ is the slope angle. The parameters *a, b* and *c* denote the distances from the front axle, rear axle, and hitch to the center of gravity (CG). Meanwhile, h_{CG} is the height of the tractor's CG from the ground, h_h is the height of the hitch from the ground, a_{x1} is the longitudinal acceleration, and a_y is the lateral acceleration of the tractor.

DERIVATION OF 5-DOF SEMITRAILER MODEL COMBINED WITH HITCH JOINT

When designing a dynamic tractor-semitrailer system, it is essential to consider the forces generated by the interaction between the vehicle's tires and the road surface. These interface forces contribute to friction, which affects the vehicle's dynamics and kinematics performance. Consequently, various tire models have been developed by researchers to accurately describe tire behavior in lateral and longitudinal slip conditions, which measures the angle between the velocity vector of the wheel and its travel direction (Ulfsjöö, 2020).

In this study, the Dugoff tire model, which incorporated both longitudinal and lateral dynamics in its formulation, was employed to calculate the tire-road force characteristics (Ribeiro et al. 2019). This model also adopted the variable of maximum road friction (μ_{max}) as presented in Equations (5) to (8), making it preponderant for estimating road friction potential and road condition estimation compared to other models, such as linear or the Fiala tire model. Additionally, the Dugoff tire model uses fewer parameters and is less reliant on accurate tire parameterization compared to sophisticated models, for instance, the Pacejka magic formula.

$$F_y = C_\alpha \left(\frac{\tan\alpha}{1+\sigma_x}\right) f(\lambda), \tag{5}$$

$$F(x) = C_\sigma \left(\frac{\sigma_x}{1+\sigma_x}\right) f(\lambda) \tag{6}$$

$$\lambda = \frac{\mu_{max} F_z (1+\sigma_x)}{2\left[\sqrt{(C_\sigma \sigma)^2 + (C_\alpha \tan\alpha)^2}\right]}, \tag{7}$$

$$f(\lambda) = \begin{cases} (2-\lambda)\lambda, if\ \lambda < 1 \\ 1, if\ \lambda \geq 1 \end{cases} \tag{8}$$

Based on the above equations, the lateral and longitudinal stiffness of tires are denoted by C_α and C_σ respectively, α represents the tire slip angle, and σ_x is the tire longitudinal slip ratio. In addition, the friction coefficient and the vertical forces were also considered. Hence, three main assumptions were made for the Dugoff tire constants, including $C_\alpha = -1.56\times10^5$ N/rad, $C_\sigma = 2.37\times10^5$ N/rad, and $\mu = 0.99$. The key assumptions in the Dugoff tire formulation are summarized as follows:

1. Small to moderate slip angles:

   For typical truck handling maneuvers, the lateral slip angles rarely exceed 10°, allowing the use of the quasi-steady Dugoff approximation.

2. Constant vertical load per wheel:

   Since the truck operated below rollover threshold conditions in the DLC and SSC tests, normal loads varied within ±10 % and were treated as constant over a short simulation interval.

3. Uniform tire–road contact patch:

   The contact area deformation was assumed to be evenly distributed, which is valid for large-diameter, stiff sidewall truck tires. These assumptions ensured computational simplicity while preserving realistic force responses, making the Dugoff model particularly suitable for heavy-vehicle simulations requiring fast dynamic evaluations.

Figure 4 illustrates the dynamic configuration of the semitrailer integrated with the proposed hitch joint model. The hitch was represented as a virtual tire element positioned at the fifth-wheel connection, where the Dugoff tire formulation computed the equivalent lateral and longitudinal forces acting between the tractor and trailer. These forces, denoted as F_{xh} and F_{xy}, were transferred through the coupling point to account for articulation effects and vertical load sharing. The virtual Dugoff tire replaced the conventional rigid hinge assumption used in prior models, thereby enabling nonlinear force interactions to be captured more realistically during cornering and transient maneuvers.

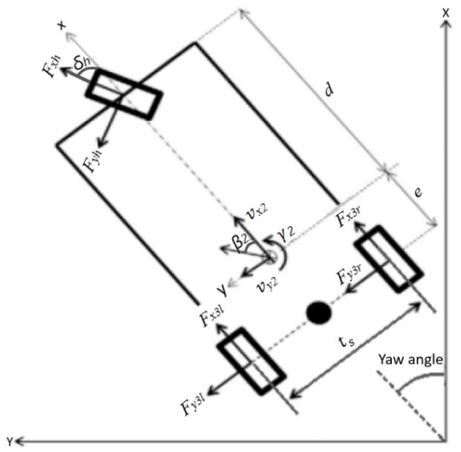

FIGURE 4. Semitrailer handling with hitch joint using Dugoff tire model

Similarly, the semitrailer free-body diagram shown in Figure 5 represented the load-transfer mechanism between the hitch and the trailer's single rear axle. The purpose of this illustration was to define the vertical equilibrium conditions used in Equations (9) to (11), where the upward

hitch reaction and rear-axle tire forces collectively balanced the trailer's total weight. This visual explanation ensured continuity between the physical configuration and the subsequent mathematical derivation.

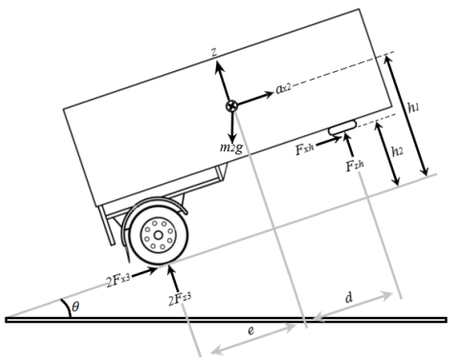

FIGURE 5. Side view of a semitrailer from an inclined ramp

Since the semitrailer had no front axle, it was fully supported by the rear axle and hitch (fifth wheel), which transferred vertical load to the tractor. Therefore, the semitrailer's entire vertical load had to be balanced between the hitch force (F_{zh}) acting upward (transmitted to the tractor), and the vertical reaction on the semitrailer's rear tires (F_{z3}). The validity of this load distribution assumption was supported by the static equilibrium analysis performed within TruckSim, where the vertical load transferred between the hitch and rear axle remained consistent with the expected range for a single-axle semitrailer. The results indicated that the model's assumption of load balance between the hitch force and tire reactions was realistic under steady-state operating conditions.

Based on this, the final equations for the semitrailer summed up the vertical reaction at the hitch connection (F_{zh}) along with the vertical force acting on the right and left tires (F_{z3r},F_{z3l}), as shown in Equations (9), (10), and (11). In these equations, m_2 is the mass of the semitrailer and a_{x2} is longitudinal acceleration. h_1 represents the height of the CG from the ground, while h_2 is the height of the hitch from the ground. Furthermore, d and e indicate the distance from the CG to the hitch and the distance from the rear tire to the CG, respectively.

SIMULATION MODEL OF TRACTOR-SEMITRAILER WITH HITCH JOINT

The complete modeling of a 3-axle tractor-semitrailer was performed in MATLAB/Simulink software, where the setup comprised several subsystems, including the load distribution model, handling model, yaw effect model, and tire longitudinal and lateral slip ratios, as displayed in Figure 6. The model also incorporated the novel fifth wheel coupling using the virtual Dugoff tire model, which could provide better handling maneuverability for the tractor-semitrailer, especially in the DLC and SSC tests that were conducted at 60 km/h for medium-speed and 90 km/h for high-speed applications (Ajorkar & He, 2025). The DLC test complied with the TruckSim software's predefined test track, based on the ISO 3888-2:2011 standard, serving to evaluate the transient response of the vehicle.

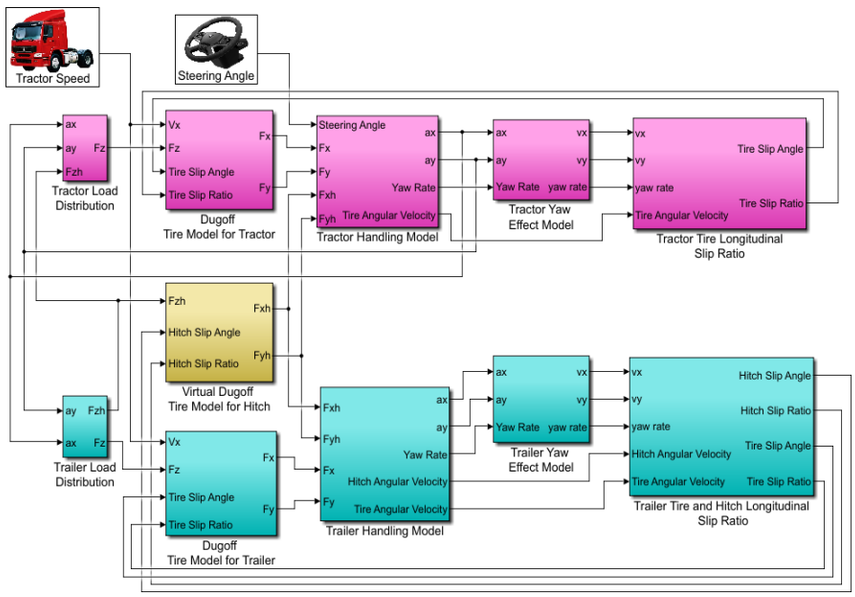

FIGURE 6. Structure of tractor-semitrailer model with hitch joint in MATLAB/Simulink

Meanwhile, the SSC test was designed in accordance with ISO 14792:2011 to assess steady-state cornering behavior (Moreno et al. 2019; Šabanovič et al. 2021). In addition, the selected test speeds aligned with the speed classification outlined in SAE J2179, which defines procedures for slow (40-60 km/h), intermediate (61-80 km/h), and high-speed (81-100 km/h) vehicle dynamics evaluations (Milani et al. 2019). Moreover, the steering wheel angle was used as the input data in the simulation, accompanied by a parameter identification process set according to the study proposed by Ta et al. (2022). All the parameters are tabulated in Table 1, showcasing the values of the variables involved in the derivation of tractor and semitrailer dynamics. On the other hand, the Heun solver with a fixed-step size of 0.01 was utilized for software configuration (Yussof et al. 2022).

TABLE 1. Simulation parameters of 3-axle tractor-semitrailer model (Ta et al. 2022)

Tractor		Semitrailer	
Parameter	Value	Parameter	Value
Mass, m_1	4404 kg	Mass, m_2	28730 kg
Yaw moment of inertia, $I_{z,t}$	8100 kg·m²	Yaw moment of inertia, $I_{z,s}$	6400 kg·m²
Track width, t_t	1.80 m	Track width, t_s	2.032 m
Distance from front axle to CG, a	1.385 m	Distance from CG to hitch, d	5.5 m
Distance from rear axle to CG, b	3.385 m	Distance from rear axle to CG, e	5.24 m
Distance from hitch to the CG, c	1.016 m	CG height from ground, h_1	2.06 m
CG height from ground, h_{CG}	1.13 m	Hitch height, h_2	1.1 m
Hitch height, h_h	1.204 m	Suspension stiffness, k_s	280 × 10³ N/m
Suspension stiffness, k_t	320 × 10³ N/m	Suspension damping, c_s	8.0 × 10³ N/m
Suspension damping, c_t	8.5 × 10³ N/m		

RESULTS AND DISCUSSION

VERIFICATION OF THE TRACTOR-SEMITRAILER MODEL WITH TRUCKSIM

In this section, the performance of the tractor-semitrailer model was evaluated by focusing on the tractor and semitrailer-hitch responses during two maneuvering tests, DLC and SSC, conducted in the TruckSim software. The steering wheel angle served as the input data when the tests were conducted at 60 km/h for medium-speed and 90 km/h for high-speed conditions. Based on this, the root mean square (RMS) value between the proposed model and the validated TruckSim model was used as the performance indicator, along with the calculation of the percentage difference of RMS to quantify the error. This was particularly relevant in the context of lateral acceleration and yaw rate, which are both critical parameters influencing vehicle stability and rollover risk. By evaluating RMS values, this study ensured that both transient and steady-state behaviors were quantitatively captured (Kumar et al. 2023).

Furthermore, the RMS-based percentage difference enabled a fair and comprehensive comparison between the proposed model and the validated TruckSim model as the reference, accounting for both the amplitude and distribution of response signals under varying speed conditions. The tractor and semitrailer responses were assessed based on lateral acceleration (a_y) and yaw rate, as both parameters affect the rollover condition, resulting in the estimation of the probability of a rollover occurrence. In addition, it was found that the concentration of force on the hitch joint also contributed to rollover; as a result, the lateral force (F_y) and vertical force (F_z) were considered in this study, while the longitudinal force (F_x) was excluded due to its negligible influence during cornering maneuvers, as verified through additional simulation observations.

PERFORMANCE EVALUATION OF TRACTOR RESPONSES DURING DLC AND SSC TESTS

As portrayed in Figures 7(a)–(b), the peak lateral acceleration recorded at a speed of 60 km/h was 0.340 g, which gradually elevated to 0.489 g at 90 km/h. These peaks occurred within the time interval of 3.788 s to 6.854 s. Additionally, the yaw rate results shown in Figures 7(c)–(d) indicated that the maximum yaw rates were 10.440 deg/s at 60 km/h and 13.133 deg/s at 90 km/h, respectively. The comparison between the proposed model and the validated TruckSim results revealed only minor discrepancies. For the DLC test, the percentage errors were 3.743%, 2.080%, 2.653%, and 1.641%, as detailed in Table 2.

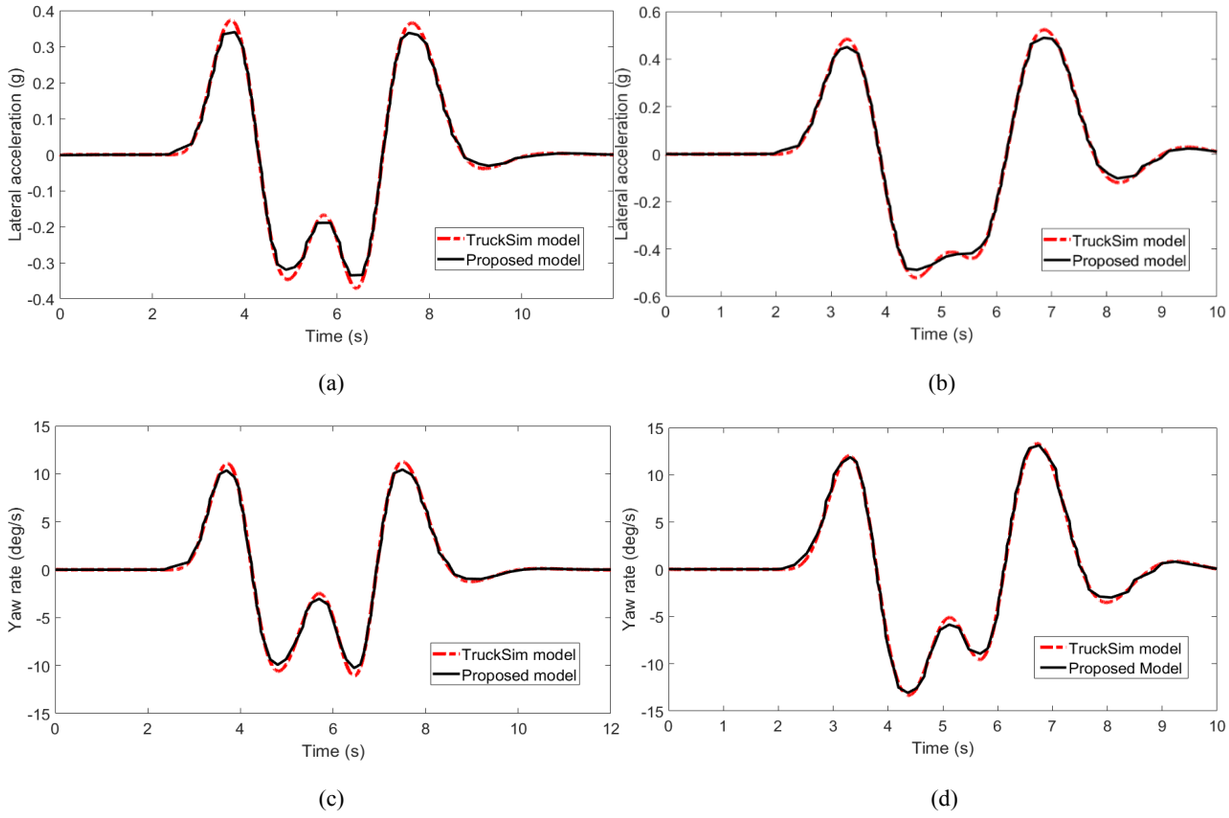

FIGURE 7. Tractor response during DLC tests; (a) Lateral acceleration at speed of 60 km/h, (b) Lateral acceleration at speed of 90 km/h, (c) Yaw rate at speed of 60 km/h and (d) Yaw rate at speed of 90 km/h

TABLE 2. Tractor model verification based on the percentage difference of RMS during the DLC test

Test	DLC		RMS		
Model	Response	Speed (km/h)	Proposed model	TruckSim	Percentage difference (%)
Tractor	Lateral acceleration (g)	60	0.196	0.203	3.473
		90	0.264	0.270	2.080
	Yaw rate (deg/s)	60	5.623	5.773	2.653
		90	6.837	6.727	1.641

Subsequently, the SSC test findings revealed satisfactory results for both lateral acceleration and yaw rate responses, based on RMS values, which highlighted the distinction between the proposed model and the validated TruckSim model. Referring to Table 3, a minimal number of errors was attained by the tractor model, 1.279% and 1.745% when accelerating from 60 km/h to 90 km/h. This outcome led to a faster time taken to reach the peak lateral acceleration of 0.312 g and 0.418 g, within a time range of 2.288 s to 2.364 s, as shown in Figures 8(e) and (f). For yaw rate, the percentage errors achieved were 1.377% and 1.615%, as presented in Figures 8(g) to (h), where the maximum yaw rates were 9.506 deg/s and 9.920 deg/s at speeds of 60 km/h and 90 km/h, respectively. Additionally, the initial onset of these responses was observed at 1.997 s and 1.689 s, as indicated in Table 3.

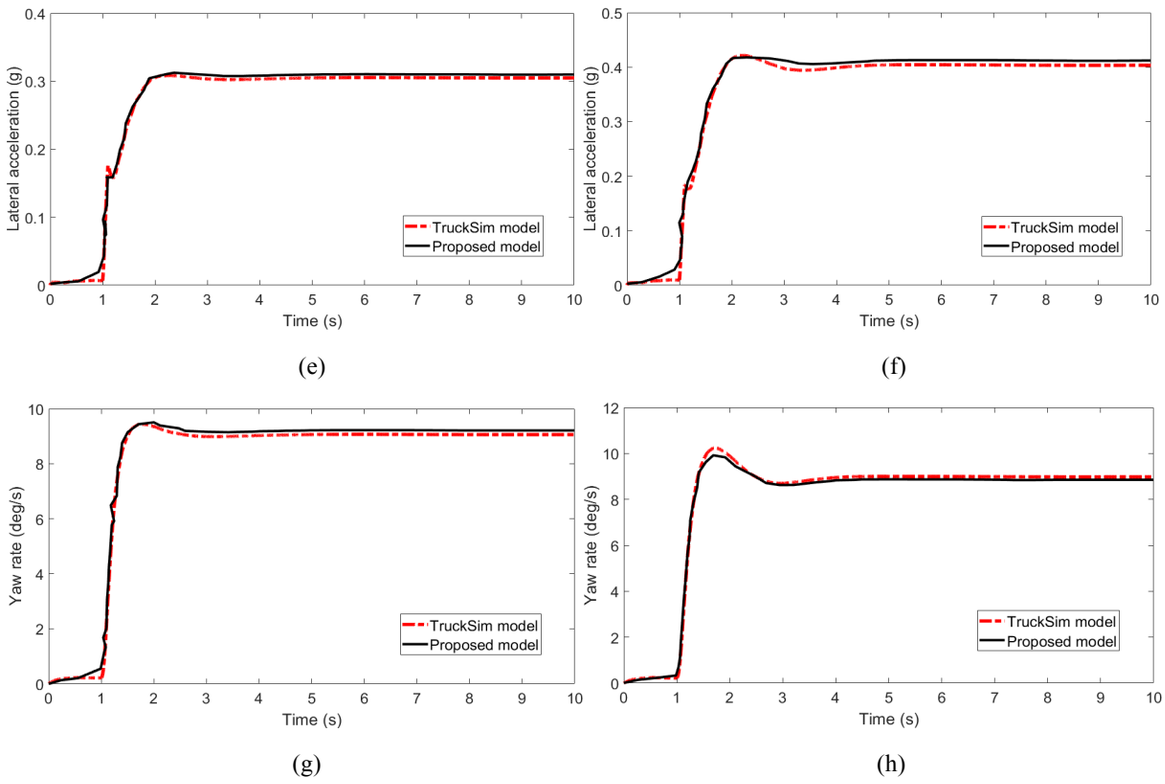

FIGURE 8. Tractor response during SSC tests; (e) Lateral acceleration at speed of 60 km/h, (f) Lateral acceleration at speed of 90 km/h, (g) Yaw rate at speed of 60 km/h and (h) Yaw rate at speed of 90 km/h

TABLE 3. Tractor model verification based on the percentage difference of RMS during the SSC test

Test Model	SSC		RMS		
	Response	Speed (km/h)	Proposed model	TruckSim	Percentage difference (%)
Tractor	Lateral acceleration (g)	60	0.261	0.258	1.279
		90	0.344	0.338	1.745
	Yaw rate (deg/s)	60	7.847	7.740	1.377
		90	7.874	8.002	1.615

PERFORMANCE EVALUATION OF SEMITRAILER-HITCH RESPONSES DURING DLC TEST

According to Figures 9(i) and 9(j), the maximum lateral acceleration generated by the trailer increased from approximately 0.219 g at 60 km/h to 0.368 g at 90 km/h. This rise was attributed to the increase in the vehicle's dynamic response, particularly the effect of higher yaw inertia as speed increased (Gillespie et al. 2021). The proposed model accurately replicated the validated TruckSim results, with percentage errors of 6.477% and 7.016% at 60 km/h and 90 km/h, respectively, as summarized in Table 4.

Additionally, Figures 9(k) and 9(l) show the yaw rate responses, where the proposed model exhibited strong agreement with the TruckSim data, with deviations of only 3.391% at 60 km/h and 5.523% at 90 km/h. The peak yaw rate increased from 7.58 deg/s to 11.86 deg/s as vehicle speed rose from 60 km/h to 90 km/h. This behavior is consistent with the findings of Li et al. (2022), who reported that vehicle yaw rate tends to rise proportionally with speed due to increased lateral forces and rotational momentum.

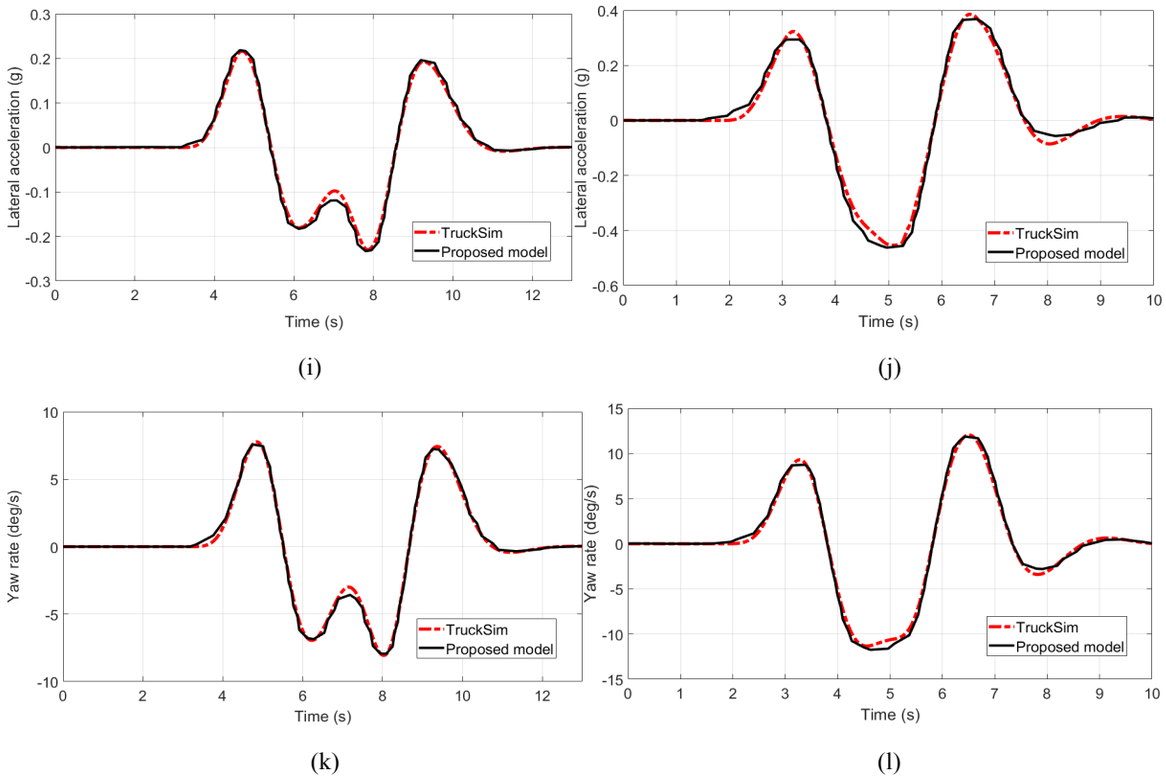

FIGURE 9. Semitrailer response during DLC tests; (i) Lateral acceleration at speed of 60 km/h, (j) Lateral acceleration at speed of 90 km/h, (k) Yaw rate at speed of 60 km/h and (l) Yaw rate at speed of 90 km/h

TABLE 4. Semitrailer and hitch models verification based on the percentage difference of RMS during the DLC test

Test Model	DLC		RMS		
	Response	Speed (km/h)	Proposed model	TruckSim	Percentage difference (%)
Semitrailer	Lateral acceleration (g)	60	0.120	0.113	6.477
		90	0.223	0.208	7.016
	Yaw rate (deg/s)	60	4.274	4.134	3.391
		90	6.059	5.742	5.523
Hitch	Lateral force (N)	60	5787.525	5564.155	4.014
		90	6198.807	6077.023	2.004
	Vertical force (N)	60	26963.611	26986.385	1.065
		90	26910.472	26929.338	1.059

The slightly higher RMS error observed for the semitrailer's lateral acceleration (less than 7%) compared to the tractor was primarily due to the higher yaw inertia and delayed response of the semitrailer body, causing greater transient oscillations and phase lag at higher speeds. Based on Arjunkumar et al. (2022), this behavior is also influenced by the articulation angle dynamics and load transfer at the hitch, which amplify discrepancies between the simplified Dugoff tire representation and the more complex TruckSim tire model. This structural difference leads to minor discrepancies in lateral force estimation under combined slip conditions, particularly at elevated speeds (Hou & Xu, 2022). Despite these differences, the overall agreement remained within acceptable limits (below 7%), demonstrating the robustness of the proposed model for dynamic simulation (Aparow et al. 2025).Figures 10(m) to 10(p) illustrate the lateral and vertical hitch forces generated by the proposed model at vehicle speeds of 60 km/h and 90 km/h. In all four scenarios, the proposed model demonstrated strong agreement with the validated TruckSim simulation results, with minimal error margins of 4.014%, 2.004%, 1.065%, and 1.059% for subplots (m),

(n), (o), and (p), respectively, as presented in Table 4. At 60 km/h, the peak lateral hitch force predicted by the proposed model was approximately 10,407.8 N, which increased to 11,616.6 N at 90 km/h. This increase reflected the heightened lateral dynamics associated with higher speeds. For the vertical hitch force, the model closely followed the TruckSim trend but exhibited a slightly dampened amplitude. The maximum vertical forces recorded were 27,796.7 N at 60 km/h and 27,706.1 N at 90 km/h. These results indicated the model's capability to accurately capture both lateral and vertical dynamic load behaviors, even under varying velocity conditions.

From a physical standpoint, the results highlighted that elevated lateral hitch forces correlated with an increased lateral load transfer ratio (LTR). In contrast, the vertical hitch force distribution can be associated with potential fatigue loading at the fifth-wheel coupling (Xue et al. 2025). An increase in lateral hitch force results in greater lateral load transfer at both the tractor's rear axle and the semitrailer's supporting axle, which are important indicators of rollover risk. The strong correlation between lateral force peaks and vehicle yaw rate responses suggests that sudden steering inputs may increase the probability of partial wheel lift, especially at higher speeds. On the other hand, variations in vertical hitch force represent cyclic load transfer through the fifth-wheel coupling, contributing to fatigue stresses in the hitch plate and kingpin assembly. In practical applications, monitoring these force components could support the development of active safety systems or fatigue life estimators that prevent rollover and structural failure during prolonged heavy-duty operations.

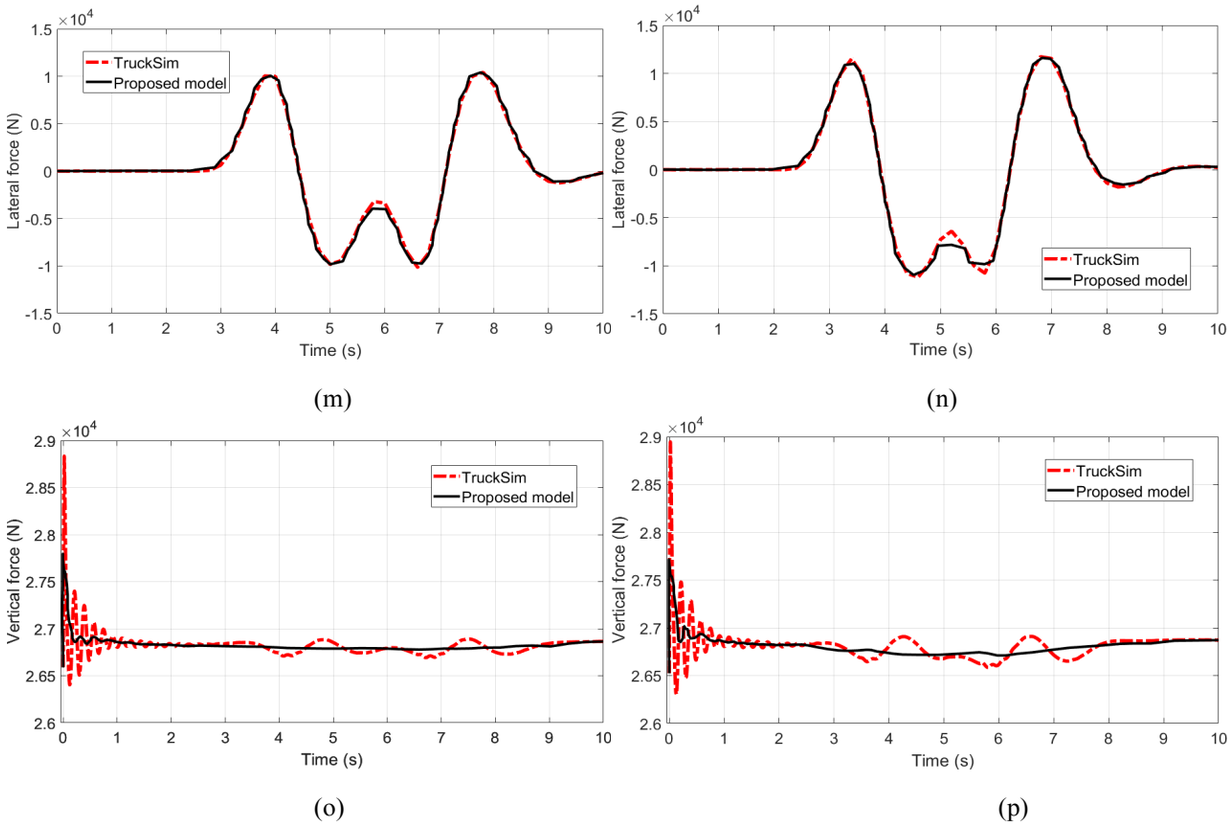

FIGURE 10. Hitch response during DLC tests; (m) Lateral force at speed of 60 km/h, (n) Lateral force at speed of 90 km/h, (o) Vertical force at speed of 60 km/h and (p) Vertical force at speed of 90 km/h

PERFORMANCE EVALUATION OF SEMITRAILER-HITCH RESPONSES DURING SSC TEST

Figure 11 illustrates the trailer's response during the SSC test, highlighting lateral acceleration and yaw rate at speeds of 60 km/h and 90 km/h. The results from the proposed model exhibited a strong resemblance to the validated TruckSim simulation outputs, with only a small percentage difference. Specifically, the lateral acceleration errors were 2.295% at 60 km/h and 1.887% at 90 km/h, while the yaw rate errors were 2.457% and 2.365%, respectively, as detailed in Table 5. As shown in Figures 11(q) to 11(t), the maximum lateral acceleration reached 0.297 g at 60 km/h and increased to 0.414 g at 90 km/h. Similarly, the peak yaw rate increased from 8.708 deg/s to 9.518 deg/s as vehicle speed increased. These peak responses occurred approximately between 2.5 s and 3 s into the maneuver, indicating the point of maximum steady-state response. The high correlation with TruckSim across all cases confirmed the validity and robustness of the proposed model under steady-state cornering conditions (Jiang et al. 2020; Yao et al. 2025).

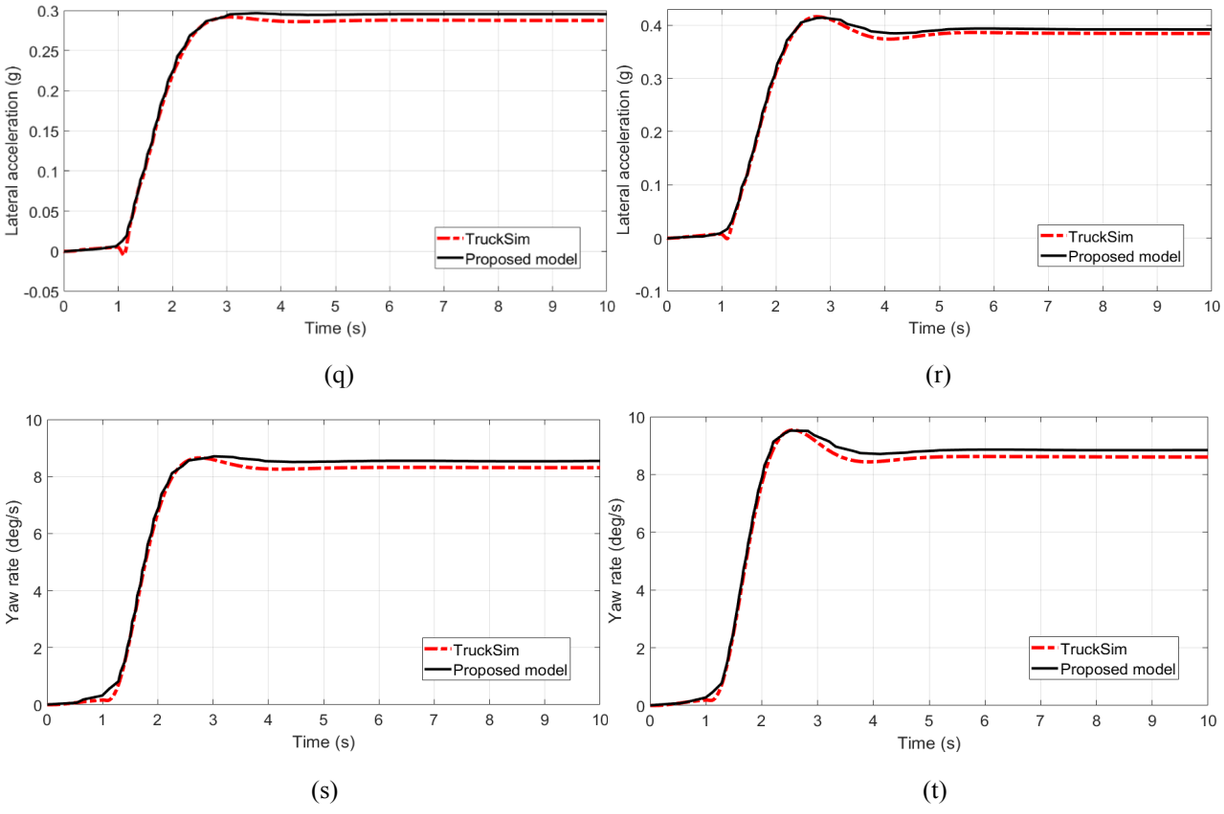

FIGURE 11. Semitrailer response during SSC tests; (q) Lateral acceleration at speed of 60 km/h, (r) Lateral acceleration at speed of 90 km/h, (s) Yaw rate at speed of 60 km/h and (t) Yaw rate at speed of 90 km/h

TABLE 5. Semitrailer and hitch models verification based on the percentage difference of RMS during the SSC test

Test Model	SSC		RMS		
	Response	Speed (km/h)	Proposed model	TruckSim	Percentage difference (%)
Semitrailer	Lateral acceleration (g)	60	0.245	0.240	2.295
		90	0.335	0.329	1.887
	Yaw rate (deg/s)	60	7.171	6.999	2.457
		90	7.446	7.274	2.365
Hitch	Lateral force (N)	60	7395.044	7168.856	3.155
		90	8718.359	8472.326	2.904
	Vertical force (N)	60	26899.030	26919.368	1.091
		90	26865.283	26885.949	1.096

The hitch force responses during the SSC test at vehicle speeds of 60 km/h and 90 km/h are presented in Figures 12(v) to 12(y). Across all four cases, the proposed model closely matched the validated TruckSim benchmark, resulting in low error values. Specifically, Figures 12(v) and 12(w) show lateral hitch forces with percentage errors of only 3.155% and 2.904%, respectively, and corresponding peak values of 8688.77 N at 60 km/h and 10,460.4 N at 90 km/h. Meanwhile, Figures 12(x) and 12(y) display the vertical hitch forces, with maximum values of 27,458.8 N at 60 km/h and slightly higher at 27,613.8 N at 90 km/h. The associated errors remained low, increasing slightly from 1.091% at 60 km/h to 1.096% at 90 km/h. These results confirmed the proposed model's capability to accurately replicate both lateral and vertical hitch dynamics under steady-state cornering conditions, with an acceptable error margin of less than 5% (Harun et al. 2019).

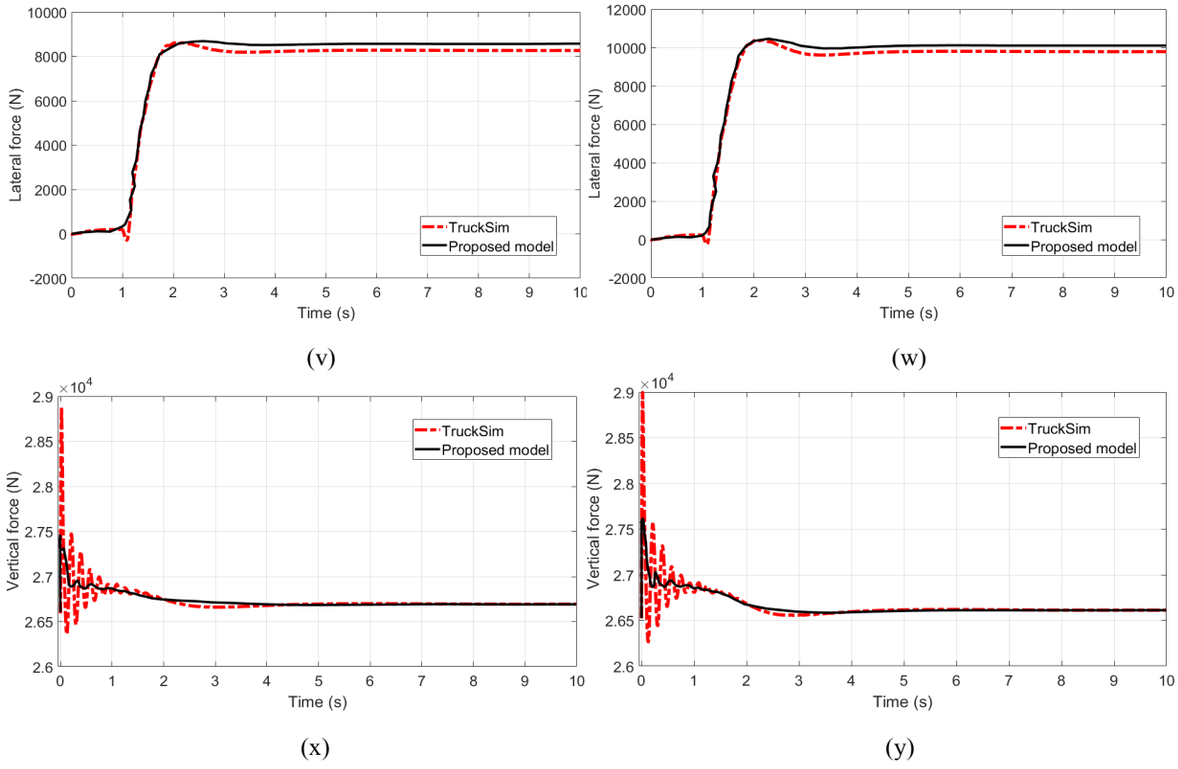

FIGURE 12. Hitch response during SSC tests; (v) Lateral force at speed of 60 km/h, (w) Lateral force at speed of 90 km/h, (x) Vertical force at speed of 60 km/h and (y) Vertical force at speed of 90 km/h

CONCLUSION

In this study, a novel hitch joint modeling approach for a tractor–semitrailer system was successfully developed by integrating the virtual Dugoff tire model. The proposed model was compared with the validated TruckSim simulations under DLC and SSC test scenarios at speeds ranging from 60 to 90 km/h. The dynamic responses, including lateral acceleration, yaw rate, and hitch forces, exhibited an average RMS percentage difference of only 2.653%, demonstrating high accuracy within acceptable limits.

Beyond numerical validation, the proposed model offers several practical contributions. Its reduced computational complexity and simplified parameterization make it suitable for integration into real-time simulation platforms, enabling heavy vehicle manufacturers to assess handling stability and rollover risks efficiently during early design stages. Moreover, the model's modular configuration allows adaptation for ADAS development, such as trailer sway mitigation or active hitch control systems, where accurate articulation dynamics are critical. It can also assist vehicle safety authorities and assessment bodies, including New Car Assessment Program for Southeast Asian Countries (ASEAN NCAP) and Malaysian Institute of Road Safety Research (MIROS), as well as international organizations such as National Highway Traffic Safety Administration (NHTSA), in developing virtual testing

frameworks for articulated vehicle stability evaluation and regulatory compliance.

For future work, the current two-dimensional model can be expanded to include three-dimensional dynamic effects, such as roll and pitch coupling, enhancing prediction accuracy under extreme loading conditions. Further improvements may involve hardware-in-the-loop (HIL) testing using actual hitch sensors and actuators to validate real-time response characteristics. Additionally, incorporating flexible body dynamics of the hitch assembly and suspension elements will allow fatigue and durability analyses, paving the way toward a comprehensive virtual testbed for articulated heavy vehicles.

ACKNOWLEDGEMENT

This project is supported by the Ministry of Higher Education Malaysia and Universiti Teknikal Malaysia Melaka (UTeM).

DECLARATION OF COMPETING INTEREST

None.

REFERENCES

Adnan, M. N. H., Kadir, Z. A., Hudha, K., Amer, N. H., Rahmat, M. S., Harun, M. H., & Aparow, V. R. 2023. Hardware-in-the-loop simulation of active roll control for single-trailer truck using steerable wheel at the middle axle. *International Journal of Heavy Vehicle Systems* 30(1): 90–118.

Ajorkar, A., & He, Y. 2025. Design of autonomous driving controls for multi-trailer articulated heavy vehicles. *Journal of Vibration and Control*.

Aparow, V. R., Pei, T. J., Vijay, R., Teng, S. S., Guerra, A. I. G., Nigel, N. Y., Ang, L., & de Boer, N. 2025. Analysis of Autonomous Emergency Steering System Using Lateral Skyhook Based Estimated Lateral Force Feedback in IPG Carmaker. *Jurnal Kejuruteraan*, 37(4), 1985–2001.

Arjunkumar, Paramhans, R., & Palanivelu, S. 2022. Yaw Stability Analysis of a Tractor Semitrailer Using Yaw Plane Model, *International Journal of Vehicle Structures and Systems* 14(2): 226-235.

Assadi, M. I., Mashhadi, B., & Bidhandi, S. K. 2024. Implementation of a Semi-active Auxiliary Axle for Lateral Stability of Articulated Heavy Vehicles at Extreme Loss of Control Limit. *International Journal of Automotive and Mechanical Engineering* 21(2): 11235-11246.

Bligh, R. P., Sheikh, N. M., Abu-Odeh, A. Y., & Kiani, M. 2021. Review and Assessment of Current Modeling Techniques in Support of Next-Generation Rollover Research—Phase I (FHWA-HRT-21-045). Federal Highway Administration (FHWA).

Gillespie, T. D., Saied Taheri, Sandu, C., & Duprey, B. L. 2021. Fundamentals of vehicle dynamics. SAE International. https://ieeexplore.ieee.org/book/9454949

Hafez, M. M. I. 2021. Investigation of integrated control of articulated heavy vehicle using scaled multi-body dynamic model. Doctoral dissertation, University of Birmingham.

Hamza, A., Dridi, I., Bousnina, K., & Ben Yahia, N. 2024. Active suspension for all-terrain vehicle with intelligent control using artificial neural networks. *Journal of Mechanical Engineering and Sciences* 18(1): 9883-9897.

Harun, M. H., Samin, P. M., K Hudha, Bakar, S. A. A., & Saad, A. M. 2019. Modelling and verification of tractor ride model. *IOP Conference Series Materials Science and Engineering*, *Malaysia* 469: 012077–012077.

Harun, M. H., Hudha, K., Samin, P. M., Bakar, S. A. A., & Kadir, Z. A. 2021. A new approach in modelling of hitch joint of a tractor semi-trailer using virtual Pacejka tyre model. *International Journal of Heavy Vehicle Systems* 28(2): 262.

Henrique, Messana, A., Carello, M., & Rosso, N. 2023. Multibody parameter estimation: a comprehensive case-study for an innovative rear suspension. *SAE Technical Papers on CD-ROM/SAE Technical Paper Series*.

Hexagon AB (2024, December 14). Adams. https://hexagon.com/products/product-groups/computer-aided-engineering-software/adams.

Hou Y., & Xu, X. 2022. High-speed lateral stability and trajectory tracking performance for a tractor-semitrailer with active trailer steering. *PloS ONE* 17(11): e0277358.

Hwang, H.-Y., Lan, T.-S., & Chen, J.-S. 2020. Developing a Strategy to Improve Handling Behaviors of a Medium-Size Electric Bus Using Active Anti-Roll Bar. *Symmetry* 12(8): 1334.

Ikhsan, N., Saifizul, A., & Ramli, R. 2021. The Effect of Vehicle and Road Conditions on Rollover of Commercial Heavy Vehicles during Cornering: A Simulation Approach. *Sustainability* 13(11): 6337.

Jiang, H., Zhou, W., Liu, C., Zhang, G., & Hu, M. 2020. Safe and Ecological Speed Control for Heavy-Duty Vehicles on Long–Steep Downhill and Sharp-Curved Roads. *Sustainability* 12(17): 6813.

Kabbani, T., Pouria Sarhadi, Ghazali, M., Gamage, C.-P., Duygu Serbes, Ersun Sozen, Ozan, B., & Ahu Ece Hartavi. 2023. Model Validation of Articulated Heavy-Duty Vehicle via IPG for Tracking Controller Design. *Transportation Research Procedia* 72: 681–687.

Kumar, A., Dheer, D. K., & Verma, S. K. 2023. An adaptive model predictive control for coupled yaw and rollover stability of vehicle during corner maneuvers. *Journal of Mechanical Engineering and Sciences* 17(4): 9764-9777.

Li, M., M.I. Ishak, & P.M. Heerwan. 2022. A numerical simulation of vehicle dynamics behavior for a four-wheel steering vehicle with the passive control system. *Journal of Mechanical Engineering and Sciences* 16(2): 8953-8964.

Linden, N. (2020, August 17). Combining multiple-body dynamics (MBD) with Finite Element Analysis (FEA). LinkedIn. https://www.linkedin.com/pulse/combining-multiple-body-dynamics-mbd-finite-element-analysis-linden

Lu, Y., Khajepour, A., Soltani, A., Wang, Y., Zhen, R., Liu, Y., & Li, G. 2023. Cab-Over-Engine truck cabins: A mathematical model for dynamics, driver comfort, and suspension analysis and control. *Proceedings of the Institution of Mechanical Engineers, Part K: Journal of Multi-Body Dynamics* 237(1): 60-73.

Milani, S., Samim Ünlüsoy, Y., Marzbani, H. & Jazar, R. 2019. Semitrailer Steering Control for Improved Articulated Vehicle Manoeuvrability and Stability. *Nonlinear Engineering* 8(1): 568-581.

Moreno, G., Vieira, R., Martins, D. 2019. Stability of Heavy Vehicles: Effect of the Road. In: Uhl, T. (Eds.), *Proceedings of the 15th IFToMM World Congress on Mechanism and Machine Science* (pp. 3585-390). Springer.

Ribeiro, A. M., Moutinho, A., Fioravanti, A. R., & de Paiva, E. C. 2019. Estimation of tire–road friction for road vehicles: a time delay neural network approach. *Journal of the Brazilian Society of Mechanical Sciences and Engineering* 42(1).

Šabanovi˘c, E., Kojis, P., Šukevi˘cius, Š., Shyrokau, B., Ivanov,V., Dhaens, M., & Skrickij, V. 2021. Feasibility of a Neural Network-Based Virtual Sensor for Vehicle Unsprung Mass Relative Velocity Estimation. *Sensors* 21: 7139.

Ta, T. H., Vo, V. H., & Duong, N. K. 2022. Study on the Dynamic Rollover Indicators of Tractor Semi-trailer Vehicle While Turning Maneuvers Based on Multibody System Dynamics Analysis and Newton-Euler Equations. In: Long, B.T., Kim, H.S., Ishizaki, K., Toan, N.D., Parinov, I.A., Kim, YH. (Eds.), *Proceedings of the International Conference on Advanced Mechanical Engineering, Automation, and Sustainable Development 2021* (pp. 30-38). Springer.

Ulfsjöö, C. H. 2020. Modeling and Lateral Control of Tractor-Trailer Vehicles during Aggressive Maneuvers. Master's Thesis, Linköping University.

Xue, H., Guo, C., Peng, X., Xu, S., Li, K., & Li, J. 2025. Collaborative Optimization on Both Weight and Fatigue Life of Fifth Wheel Based on Hybrid Random Forest with Improved BP Algorithm. *Applied Sciences* 15(7), 4006.

Yao, J., Qu, W., Tian, D., Shi, J., Wang, J., Xu, B., & Wang, S. 2025. Optimization control of all-terrain rescue lift vehicle safety performance based on state feedback. *PLoS ONE* 20(5): e0323293–e0323293.

Yussof, M. A. M., Amer, N. H., Kadir, Z. A., Hudha, K., Rahmat, M. S., & Harun, M. H. 2022. Yaw stability control of single-trailer truck using steerable wheel at middle axle: hardware-in-the-loop simulation. *International Journal of Dynamics and Control* 10(6): 2072–2094.

Zainuddin, N. I., Arshad, A. K., Hashim, W., & Hamidun, R. 2023. Heavy Goods Vehicle: Review of Studies Involving Accident Factors. *Jurnal Kejuruteraan* 35(1): 3–12.